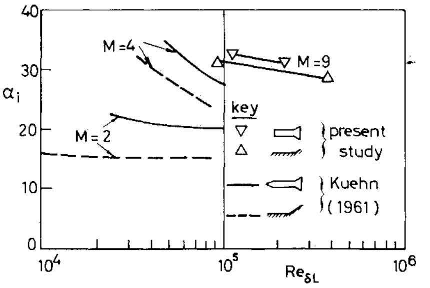

Fig. 3 Comparison of axisymmetric and planar two-dimensional incipient separation results.

separation angle (α_i) could be determined from the disappearance of the pressure overshoot downstream of reattachment on the wedge. This criterion is less reliable for the axisymmetric case because the attached flow pressure distribution is already of this form with a locally two-dimensional pressure rise at the corner followed by a gradual decay to the cone value far downstream on the flare.

Incipient separation was determined here by three methods which had given good agreement for the two-dimensional configuration.[4,5] These were 1) looking for the onset of an increase in pressure and heat-transfer rate ahead of the flare; 2) looking for a change in the shape of the pressure and heat-transfer distributions on the flare; and 3) by plotting the separation length (l) as measured from schlieren photographs, against flare angle and extrapolating to $l = 0$. The answers from these three methods agreed to within $\frac{1}{2}°$. The results (Fig. 3) are compared with the wedge compression corner experiments of Elfstrom and Coleman.[4,6] The results of Kuehn[2] for Mach numbers of 2 and 4 are also shown. All of the data exhibit the trend of decreasing α_i with increasing Re_{δ_L} where δ_L is the undisturbed boundary-layer thickness at the cylinder-flare junction. This is opposite to the trend noted by Rose, Page, and Childs in their nozzle wall experiments and may be the result of different upstream histories of the boundary layers in the two cases.

Data are presented by Rose, Page, and Childs[1] "which indicate that separation occurs in axially symmetric flows at much lower pressure rises than would be expected on the basis of previous data for planar two-dimensional flows." This conclusion is in direct contrast to the information given here and to that given by Kuehn,[2] both of which compare planar and axisymmetric external flows. Either there is a great difference between incipient separation on internal and external surfaces, or the determination of incipient separation is very sensitive to the detection method employed, as found for example by Spaid and Frishett.[7] From a practical viewpoint, the designer needs to know when significant changes in pressure and heat-transfer rate distributions will occur as a result of separation so there is considerable merit in using such measurements to define incipient separation whenever possible.

To summarize, our results have shown that for axisymmetric external flow the incipient separation angle is slightly higher than for the planar two-dimensional case. There is a close similarity between the surface pressure and heat transfer rate distributions for the two cases.

References

[1] Rose, W. C., Page, R. J., and Childs, M. E., "Incipient Separation Pressure Rise for a Mach 3.8 Turbulent Boundary Layer," *AIAA Journal*, Vol. 11, No. 5, May 1973, pp. 761–763.

[2] Kuehn, D. M., "Turbulent Boundary Layer Separation Induced by Flares on Cylinders at Zero Angle of Attack," TR R-117, 1961, NASA.

[3] Needham, D. A., Elfstrom, G. M., and Stollery, J. L. "Design and Operation of the Imperial College No. 2 Hypersonic Gun Tunnel," Aero Rept. 70-04, 1970, Imperial College, London, England.

[4] Coleman, G. T., "Hypersonic Turbulent Boundary Layer Studies," Ph.D. thesis, 1973, Dept. of Aeronautics, Imperial College, Univ. of London, London, England.

[5] Elfstrom, G. M., "Turbulent Hypersonic Flow at a Wedge Compression Corner," *Journal of Fluid Mechanics*, Vol. 53, Pt. 1, 1972, pp. 113–127.

[6] Coleman, G. T. and Stollery, J. L., "Heat Transfer from Hypersonic Turbulent Flow at a Wedge Compression Corner," *Journal of Fluid Mechanics*, Vol. 56, Pt. 4, 1972, pp. 741–752.

[7] Spaid, F. W. and Frishett, J. C., "Incipient Separation of a Supersonic Turbulent Boundary Layer, Including Effects of Heat Transfer," *AIAA Journal*, Vol. 10, No. 7, July 1972, pp. 915–922.

Strong Spherical Blast Waves in a Dust-Laden Gas

NATHAN GERBER* AND JOAN M. BARTOS†
Ballistic Research Laboratories,
Aberdeen Proving Ground, Md.

Nomenclature

C_D = drag coefficient (gas flow drag on dust particle; based on cross-sectional area of sphere)
E_o = energy of blast, joules (sphere); joules/m (cylinder)
M' = $|v_p - v|(\gamma p/\rho)^{-1/2}$—Mach number of flow relative to dust
p = gas pressure, N/m^2
r = spatial coordinate measured from center of blast, m
r_p = coordinate of dust particle, m
$r_{p\,\min}$ = coordinate of inner boundary of dust layer, m
R_s = coordinate of shock wave, m
R_{s_1} = initial value of r_p for a particle trajectory, m
Re' = $2\rho|v - v_p|\sigma_p/\mu$—Reynolds number based on flow relative to dust
t = time, sec
t_1 = time when shock reaches particle located at R_{s1}, sec
T, T_p = gas temperature, dust particle temperature, °K
v, v_p = gas velocity, dust particle velocity, m/sec
γ = ratio of specific heats of gas
μ = viscosity coefficient, kg/(m sec)
ρ, ρ_p = gas density, material density of dust particle, kg/m^3
σ_p = radius of spherical dust particle, m

Subscript

∞ = initial undisturbed condition

Statement of Problem

WHEN a blast wave passes through a dust-laden gas, the ensuing motion of the dust particles may produce noticeable effects on the loading and abrasion experienced by structures in the vicinity of the explosion. This Note discusses a simplified treatment of the two-phase flow produced by a spherical blast wave traveling through a uniform dust-laden gas.‡ The assumptions made here permit us to neglect interaction of particles and the effect of the particles on the gas flow; the problem reduces then to the computation of trajectories of individual dust particles (considered point masses) in a known unsteady flowfield.

The following assumptions are made for the dust: 1) the particles are spheres of uniform size and material density,

Received July 26, 1973.
Index categories: Multiphase Flows; Shock Waves and Detonations; Supersonic and Hypersonic Flow.

* Aerospace Research Engineer, Exterior Ballistics Laboratory.
† Mathematician, Exterior Ballistics Laboratory.

‡ A more detailed account is found in Ref. 1.

initially at rest; 2) the volume and spatial density (mass per unit volume of solid-gas mixture) of the dust particles are small compared to the corresponding volume and density of the gas; and 3) the heat transfer between the gas and the dust has a negligible effect on the drag coefficient, C_D, of the flow relative to a particle.

The motion of a spherical particle acted upon solely by an aerodynamic drag force can be described by

$$\begin{aligned} dv_p/dt &= \tfrac{3}{8}(\rho/\rho_p)(C_D/\sigma_p)\left|v-v_p\right|(v-v_p) \\ dr_p/dt &= v_p \end{aligned} \tag{1}$$

where ρ and v are known flow variables. A particle located at $r = R_{s_1}$ will remain stationary until the spherical shock wave reaches it at time $t = t_1$; t_1 is obtainable from the known shock trajectory. With instantaneous passage of the shock, the initial conditions for Eq. (1) are: $r_p = R_{s_1}$ and $v_p = 0$ at $t = t_1$.

The drag coefficient, C_D, should be prescribed as accurately as possible in terms of M' and Re'. Here we use C_D from a recent compilation[2] of empirical data on sphere drag which is applicable in the regime $0.1 < M' < 6.0$ and $20 < Re' < 10^6$ for $T_p/T = 1$. The data[2] indicate that when $Re' > 10^6$, $C_D = C_D$ $(M', Re' = 10^6)$ is a reasonably accurate approximation. For $M' < 0.2$ and/or $Re' < 200$, we apply the empirical formula of Crowe[3] for drag coefficient (with $T_p/T = 1$).

In providing flow variables for Eq. (1) we confine this study to a simple model of flow produced by a spherical blast, namely, self-similar flow. Self-similar flow solutions are available in Refs. 4 and 5, which treat the subject in detail. The basic assumptions are: 1) a finite quantity of energy, E_o, is instantaneously deposited at a point, giving rise to a spherically expanding shock wave; 2) the shock wave is strong enough so that the ambient atmospheric pressure is neglected ($p_\infty = 0$); 3) the gas inside the shock is an inviscid ideal gas, with adiabatic exponent γ.

Some of the assumptions above are violated in the course of the history of the unsteady two-phase flow (e.g., occurrence of dense concentrations of dust particles, invalidity of strong shock assumption far from the center of blast). Nevertheless, we still expect our calculations to show the qualitative nature of the physical phenomenon at early times.

Calculations

Calculations show that momentum imparted to a dust particle by the gas flow behind an attenuating shock enables the particle eventually to attain a speed greater than that of the local flow; then the particle experiences a decelerating rather than accelerating influence from the gas.

Figure 1 shows the drag coefficient-time history for three

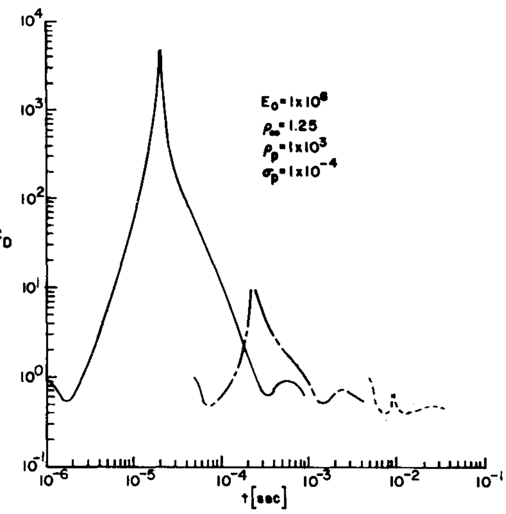

Fig. 1 Drag coefficient history of dust particles in spherical blast.

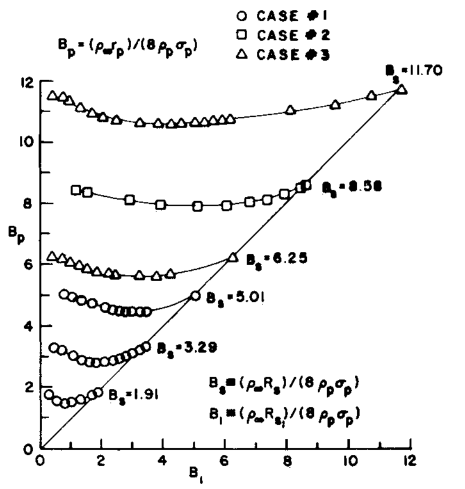

Fig. 2 Distribution of dust particles in spherical blast.

dust particles at different distances from the blast center, after the passage of a spherical blast. The major point to be noted is that C_D is always finite, except possibly at the sharp peaks (when the particle velocity reaches and exceeds the local flow velocity). The conclusion here is that there is practically always a velocity lag between the dust particles and the gas, and consequently these particles cannot be assumed to be without inertia. The conditions considered here then will not be applicable to the situations treated in Refs. 6 and 7, which consider the particles to be in equilibrium with the flow, i.e., $C_D = \infty$.

Particle trajectories were computed for six "cases"; i.e., six sets of E_o, ρ_∞, ρ_p, and σ_p; parameter values are listed in Fig. 3. In each case trajectories were computed for many particles, i.e., values of R_{s_1}. For a given shock location the distribution of dust particles can be obtained from these calculations.

Figure 2 shows six typical particle distribution curves in terms of nondimensional quantities. Each curve shows the locations of all the entrained particles at a fixed time, corresponding to the given B_s. The presence of a minimum on a curve demonstrates that all particles, at the time given, are displaced further than a certain radius $r_{p\,\min}$. This situation implies that all the particles affected by the blast are contained in a dust layer right behind the spherical shock, leaving an inner dust-free core of gas.

Data Correlation

In seeking to correlate results of trajectory computations, we turn to an approximate model[1] which is a further simplification of self-similar flow.§ The additional assumptions made in the approximate model are 1) the flow within the sphere is divided into two regions: a) a region immediately behind the shock, of thickness Δ, which contains all the mass, and b) an inner layer, in which the drag on the particle is neglected; 2) the thickness Δ is small compared to R_s; 3) the gas density and velocity are constant across the outer layer, the latter taken as the value right behind the shock; 4) drag coefficient, C_D, is a constant, the same value for all trajectories.

It is then possible to integrate Eq. (1) analytically. The resulting closed form solution yields the following conclusions: 1) there is a dust layer right behind the shock-wave and a dust-free inner core; 2) the ratio of dust layer thickness to shock radius is completely determined by the single parameter combination, $B_s = (\rho_\infty R_s)/(8\sigma_p\rho_p)$ (in fact, the ratio is a monotonically decreasing function of B_s, approaching a small but finite value as the latter goes to infinity); 3) dust particles originally very near the center of the blast overtake and pass the decelerating spherical shock wave.

§ This is based on the approximate model employed in Ref. 8.

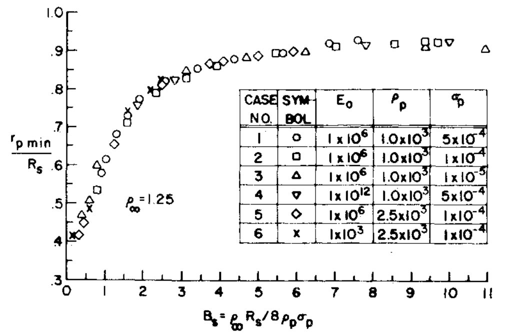

CASE NO.	SYMBOL	E_0	ρ_p	σ_p
1	○	1×10^6	1.0×10^3	5×10^{-4}
2	□	1×10^6	1.0×10^3	1×10^{-4}
3	△	1×10^6	1.0×10^3	1×10^{-5}
4	▽	1×10^{12}	1.0×10^3	5×10^{-4}
5	◇	1×10^6	2.5×10^3	1×10^{-4}
6	×	1×10^3	2.5×10^3	1×10^{-4}

Fig. 3 Relative thickness of dust-free core in spherical blast.

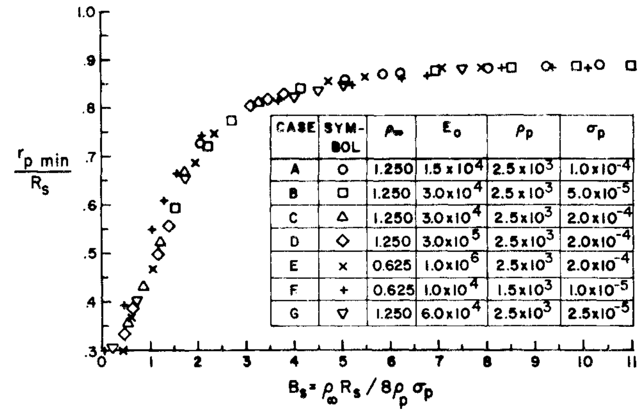

CASE	SYMBOL	ρ_∞	E_0	ρ_p	σ_p
A	○	1.250	1.5×10^4	2.5×10^3	1.0×10^{-4}
B	□	1.250	3.0×10^4	2.5×10^3	5.0×10^{-5}
C	△	1.250	3.0×10^4	2.5×10^3	2.0×10^{-4}
D	◇	1.250	3.0×10^5	2.5×10^3	2.0×10^{-4}
E	×	0.625	1.0×10^6	2.5×10^3	2.0×10^{-4}
F	+	0.625	1.0×10^4	1.5×10^3	1.0×10^{-5}
G	▽	1.250	6.0×10^4	2.5×10^3	2.5×10^{-5}

Fig. 4 Relative thickness of dust-free core in cylindrical blast.

We now use the second conclusion as a guide to correlate the results from numerical integration of Eq. (1) with the self-similar flow. Figure 3 shows many values of $r_{p\,\min}/R_s$ computed for the six listed cases. The data correlate quite well, in agreement with prediction of the approximate model. Thus a single curve predicts relative dust layer thickness in terms of a combination of the basic parameters of the problem, at least for air initially at "standard density." Furthermore, $r_{p\,\min}/R_s$ increases monotonically, approaching a value less than unity with increasing B_s; and particles located initially very near the center of blast are found to overtake and pass the shock wave.

The very same treatment just described is also applicable to the cylindrical blast, taking geometrical differences into account. The dust layer thickness data are plotted in Fig. 4 for the cylindrical blast.

Discussion

The ambient pressure, p_∞, does not enter the problem because of the self-similar flow. Also, E_o does not appear as a parameter when the ratio of dust layer thickness to shock radius is given as a function of shock radius (Figs. 3 and 4). With a more accurate flow model these quantities would most likely appear in any correlation of computational results.

Generally, dust particles in the air will be diverse in size and material density; still, a dust layer and a dust-free core will be produced by an explosion. Under the foregoing assumptions, each particle can be treated separately; thus for given ρ_p, the inner edge of the layer will be formed with the largest particles, according to Fig. 3.

It was demonstrated that the flow produced by an explosion could accelerate stationary particles to overtake the expanding shock. One can expect that explosion products (e.g., unburned powder particles) injected into this flow with finite velocity could also overtake the shock front.

References

[1] Gerber, N. and Bartos, J. M., "Effect of Strong Blast Wave on a Dust-Laden Gas," Ballistic Research Laboratories Report, to be published.

[2] Bailey, A. B. and Hiatt, J., "Free-Flight Measurements of Sphere Drag at Subsonic, Transonic, Supersonic, and Hypersonic Speeds for Continuum, Transition, and Near-Free-Molecular Flow Conditions," AEDC-TR-70-291, March 1971, Arnold Engineering Development Center, Tullahoma, Tenn.

[3] Crowe, C. T., "Drag Coefficient of Particles in a Rocket Nozzle," *AIAA Journal*, Vol. 5, No. 5, May 1967, pp. 1021–1022.

[4] Sedov, L. I., *Similarity and Dimensional Methods in Mechanics*, Academic Press, New York, 1959.

[5] Sakurai, A., "Blast Wave Theory," *Basic Developments in Fluid Dynamics*, Vol. 1, edited by M. Holt, Academic Press, New York, 1965.

[6] Sidorkina, S. I., "On Certain Motions of Aerosols," *Doklady Akademii Nauk SSSR*, Vol. 112, No. 3, 1957.

[7] Dewey, J. M., "The Properties of a Blast Wave Obtained from an Analysis of the Particle Trajectories," *Proceedings of the Royal Society of London*, Ser. A, Vol. 324, No. 1558, 1971, pp. 275–299.

[8] Spurk, J. H. and Gerber, N., "Dust Collection Efficiency for Power Law Bodies in Hypersonic Flight," *AIAA Journal*, Vol. 10., No. 6, June 1972, pp. 755–761.